Free Radical Biology and Medicine 67 (2014) 103–114

Contents lists available at ScienceDirect

Free Radical Biology and Medicine

journal homepage: www.elsevier.com/locate/freeradbiomed

Original Contributions

Glutathione is essential to preserve nuclear function and cell survival under oxidative stress

Elie Hatem [a,b,c], Véronique Berthonaud [a,b,c], Michèle Dardalhon [d], Gilles Lagniel [a,b,c], Peggy Baudouin-Cornu [a,b,c], Meng-Er Huang [d], Jean Labarre [a,b,c], Stéphane Chédin [a,b,c,*]

[a] CEA, iBiTecS, F-91191 Gif-sur-Yvette, France
[b] CNRS, FRE3377, F-91191 Gif-sur-Yvette, France
[c] Université Paris-Sud, FRE3377, F-91191 Gif-sur-Yvette, France
[d] CNRS, Institut Curie, UMR3348 "Genotoxic Stress and Cancer," F-91405 Orsay, France

ARTICLE INFO

Article history:
Received 10 July 2013
Received in revised form
8 October 2013
Accepted 12 October 2013
Available online 18 October 2013

Keywords:
GSH
Nuclear function
Oxidative stress response
Protein carbonylation
Starvation
H_2O_2
Free radicals

ABSTRACT

Glutathione (GSH) is considered the most important redox buffer of the cell. To better characterize its essential function during oxidative stress conditions, we studied the physiological response of H_2O_2-treated yeast cells containing various amounts of GSH. We showed that the transcriptional response of GSH-depleted cells is severely impaired, despite an efficient nuclear accumulation of the transcription factor Yap1. Moreover, oxidative stress generates high genome instability in GSH-depleted cells, but does not activate the checkpoint kinase Rad53. Surprisingly, scarce amounts of intracellular GSH are sufficient to preserve cell viability under H_2O_2 treatment. In these cells, oxidative stress still causes the accumulation of oxidized proteins and the inactivation of the translational activity, but nuclear components and activities are protected against oxidative injury. We conclude that the essential role of GSH is to preserve nuclear function, allowing cell survival and growth resumption after oxidative stress release. We propose that cytosolic proteins are part of a protective machinery that shields the nucleus by scavenging reactive oxygen species before they can cross the nuclear membrane.

Introduction

Organisms growing in an aerobic environment must cope with reactive oxygen species (ROS) such as superoxide ($O_2^{\bullet -}$), hydrogen peroxide (H_2O_2), and hydroxyl radical ($HO^{\bullet}$). In particular, mitochondria generate $O_2^{\bullet -}$ that is dismutated to H_2O_2 by the manganese superoxide dismutase [1–3]. In a process known as the Fenton reaction, H_2O_2 reacts with Fe^{2+} and produces $HO^{\bullet}$, one of the most reactive oxidants in nature [4]. ROS damage all the cellular macromolecules, especially proteins, because they can introduce modifications in the side chain of amino acids. These modifications can be irreversible, such as the introduction of carbonyl groups into the side chain of particular amino acids (i.e., arginine, lysine, proline, and threonine). The so-called carbonylation process causes protein dysfunction [5] and protein aggregation, leading to their accumulation during oxidative stress [6,7]. Because carbonylated amino acids are now easily detectable, protein carbonylation has emerged as a general biomarker of protein oxidation [8,9]. The consequences of in vivo protein carbonylation have been studied in many different organisms, and it is well established that their accumulation is tightly associated with numerous diseases (e.g., Alzheimer and Parkinson diseases, diabetes, and cancer) and is linked to aging processes [10–12]. Importantly, recent reports have suggested that protein carbonylation could be a cause, rather than a consequence, of cellular death [13]. In particular, it was proposed that γ and UV irradiation would induce cellular mortality of bacteria through the carbonylation of enzymes involved in DNA repair [14].

ROS also play a central role in a range of biological processes, including signaling [15], which requires a tight control of their abundance. Redox homeostasis is achieved by antioxidant systems that scavenge or degrade the ROS produced endogenously at low levels during cell growth [16]. In the yeast *Saccharomyces cerevisiae*, H_2O_2 homeostasis involves a large collection of enzymes [4]: two catalases (Ctt1 and Cta1), five peroxiredoxins (Tsa1, Tsa2, Ahp1, Dot5, and Prx1), and three glutathione peroxidases (Gpx1, Gpx2, and Gpx3). However, these constitutive antioxidant machineries can be rapidly overwhelmed by exogenous oxidative conditions, and cells have developed mechanisms of response that lead to the induction of oxidative stress-responsive enzymes. In *S. cerevisiae*, oxidative stress sensing triggers the nuclear accumulation of transcription factors, some being stress specific (e.g., Yap1 [17]), others being activated under a wide variety of stress conditions (e.g., Msn2/4 [18]). The physiological response to

* Corresponding author.
E-mail address: stephane.chedin@cea.fr (S. Chédin).

0891-5849/$ - see front matter © 2013 Elsevier Inc. All rights reserved.
http://dx.doi.org/10.1016/j.freeradbiomed.2013.10.807

H_2O_2 treatment changes the expression of at least 167 proteins [19]: antioxidant enzymes are highly induced, whereas expression of the majority of other proteins is strongly downregulated. This deep reorganization of genomic expression allows a dedicated response to rapid changes in the cellular environment.

In addition to the enzymatic protection against ROS, cells also contain small antioxidant molecules, such as glutathione (GSH). With an intracellular concentration between 1 and 10 mM, GSH is the most abundant nonprotein thiol in the cell and is considered the major redox buffer of the cell [20–22]. This tripeptide is synthesized via a two-step process [23]: the γ-glutamylcysteine synthetase (Gsh1) generates γ-glutamylcysteine (γ-GC) from cysteine and glutamate, and the glutathione synthetase adds a glycine on the γ-GC to form a molecule of GSH [24]. We have shown that, in *S. cerevisiae,* the intracellular concentration of GSH is not exclusively controlled at the synthesis level, because GSH degradation also plays a major role. In particular, during sulfur starvation, degradation of GSH into cysteine, from which are synthesized the sulfur-containing compounds required for cellular growth, is strongly increased [25]. However, a high concentration of GSH is not strictly essential for yeast cell division. For instance, Δ*gsh1* mutant cells, unable to synthesize GSH, can grow in the absence of additional GSH in the culture medium for 8 to 10 generations [26,27]. This demonstrates that a very low concentration of GSH is sufficient for cell viability. It is noteworthy that the essential role of GSH is not to buffer the redox equilibrium of the cell. Indeed, anaerobia does not improve the growth of Δ*gsh1* mutant cells depleted of GSH [27]. Sipos et al. [28] provided the first evidence that GSH is involved in the maturation of cytoplasmic Fe/S-containing proteins. More recently, it has been shown that GSH is required for the maintenance of mitochondrial DNA and that GSH depletion in Δ*gsh1* cells triggers an iron starvation-like response [29]. This observation was confirmed by Kumar et al. [30], who suggested that a high concentration of GSH serves as a backup to the thioredoxin pathway, whereas scarce amounts of GSH are required to ensure its vital function in iron metabolism.

GSH-depleted Δ*gsh1* cells are hypersensitive to H_2O_2 treatment [20,31], but the consequence of GSH depletion during oxidative stress has never been clarified. To address this question, we used *S. cerevisiae* to characterize the physiological response to H_2O_2 treatment both in wild-type (WT) cells grown under sulfur starvation and in Δ*gsh1* cells grown under GSH depletion. We observed that a very low concentration of GSH led to the accumulation of carbonylated proteins and cell lethality during oxidative stress. We identified a minimal GSH concentration that preserved cells from H_2O_2-induced death without protecting proteins against oxidative damage. In these cells, the translational activity was strongly repressed by H_2O_2 treatment, suggesting that the induction of stress-responsive enzymes was not strictly required to maintain cell viability. In contrast, further analyses revealed that this minimal concentration of GSH was sufficient to protect nuclear DNA and nuclear function against oxidative damage. This protection appeared to be an essential parameter of cell survival during H_2O_2 treatment.

Materials and methods

Strains and growth conditions

Yeast strains used in this study derived from the BY4742 background (Euroscarf) (Supplementary Table SI). Primers used to construct the YAP1-GFP chimeric chromosomic gene were designed according to Longtine et al. [32] (Supplementary Table SII). BY4742 (WT) cells were grown at 30 °C to $A_{600\ nm}=0.4$ (midexponential phase, 1.7×10^7 cells/ml) in an S100 minimal medium containing 100 μM $(NH_4)_2SO_4$ [25] and supplemented with the appropriate amino acids. To induce sulfur starvation, yeast cells were grown in S100 medium, centrifuged (4000 rpm, 5 min, 30 °C), and the pellet was suspended for an extra hour in S0 medium, which is S100 medium without $(NH_4)_2SO_4$ [25]. Δ*gsh1* cells were grown in S100 medium, supplemented with the appropriate amino acids + 100 μM GSH (Sigma–Aldrich) to $A_{600\ nm}=0.4$ (midexponential phase, 1.7×10^7 cells/ml). For GSH depletion, Δ*gsh1* cells were grown in S100 + 100 μM GSH medium to $A_{600\ nm}=0.4$. After centrifugation (4000 rpm, 5 min, 30 °C), the pellet was diluted in S100 medium and the growth was resumed for three to eight generations.

For all experiments, oxidative stress was induced by adding 400 μM H_2O_2 (Sigma–Aldrich) to the culture medium.

For survival assays, cells were grown under normal or deprived conditions before addition of 400 μM H_2O_2. At $t=0$, 20, and 60 min, cells were harvested and diluted samples were plated onto S100 + 100 μM GSH + 0.8% agarose solid medium. Viability was assessed by counting the colony-forming units after 3 days at 30 °C.

Fluorescence microscopy experiments

Yeast cells (8.5×10^7), grown under the various conditions, were harvested by centrifugation and fixed for 5 min at room temperature in 5 ml of 4% formaldehyde in phosphate-buffered saline (PBS). Cells were washed with PBS and nuclei were stained by adding 4,6-diamidino-2-phenylindole (DAPI) to a final concentration of 50 μg/ml. Microscopy observations were done using a DMIRE2 Leica microscope (63 × /1.4 oil immersion objective).

Iron and GSH quantification, H_2O_2 consumption rate

Iron quantification were performed on 42.5×10^7 yeast cells as previously described [33].

For estimation of the labile iron pool, calcein was used as described [34]. Cell fluorescence was assessed using a DMIRE2 Leica microscope (63 × /1.4 oil immersion objective) and the fluorescence level was measured by image quantification using the ImageJ public software.

For total GSH quantification, 8.5×10^7 yeast cells grown under the various conditions were harvested, washed with ice-cold water, suspended in 0.1% perchloric acid, and boiled for 5 min at 95 °C. After centrifugation (13,000 rpm, 1 min, room temperature), 7 μl of the supernatant was diluted three times in 0.1 M potassium phosphate buffer, pH 7.5, 5 mM EDTA. GSH was then quantified according to Rahman et al. [35]. GSH concentration was calculated by assuming that the volume of an individual cell is 4.5×10^{-14} L [30].

Hydrogen peroxide degradation rate was assessed as described [36]. The first-order rate constants were deduced from values of H_2O_2 remaining in the culture medium fitted with exponential curves. Results are given in min^{-1} for 1.7×10^7 cells/ml.

RNA extraction and RT-PCR

Total RNA extraction and RT-PCR were performed as described [37] using iQ5 real-time PCR detection systems and MESA Green qPCR Master Mix Plus for SYBR Assay (Eurogentec). Gene expression was calculated as described [38]. See Supplementary Table SII for primer sequences.

Protein analyses

For carbonylated protein detection, 25.5×10^7 yeast cells were harvested from the various growth conditions. They were washed twice in water and suspended in 200 μl lysis buffer (50 mM Hepes, 100 mM KCl, 10% glycerol, 1.25 mM phenylmethanesulfonyl

fluoride, and 1 × Complete EDTA-free; Roche). Two hundred microliters of glass beads (Sigma–Aldrich) was added and the cells were lysed by vortexing (45 min, 4 °C). After centrifugation (15,000 rpm, 15 min, 4 °C), supernatants were collected and protein concentration was determined. For derivatization [39], the volume of 25 μg of proteins was adjusted to 60 μl in 1 × PBS and 6% sodium dodecyl sulfate. 2,4-Dinitrophenylhydrazine (DNPH) solution (60 μl; 4 mM DNPH (Sigma–Aldrich) in 5% trifluoroacetic acid) was added and samples were incubated for 30 min at 20 °C. The reaction was stopped by adding 120 μl Stop solution (0.6 M Tris-base, 5.5% 2-mercaptoethanol) and proteins were precipitated for 45 min by adding 4 volumes of ice-cold acetone. After centrifugation (14,000 rpm, 15 min, 4 °C), the protein pellet was washed with ice-cold acetone and dried and proteins were suspended in Laemmli buffer [40]. Twelve micrograms of each sample was analyzed by SDS–PAGE and derivatized proteins were revealed by Western blot using a rabbit anti-DNP antibody (Sigma–Aldrich). Semiquantitative analyses were performed with the Odyssey scanner (Li-Cor).

Rad53 phosphorylation was analyzed as previously described [41] using a goat anti-Rad53 antibody (RAD53 (yC-19); Santa Cruz Biotechnology).

Histones were purified from 1 L of Δ*gsh1* cell culture as described [42].

Polysome profiling

For each condition, 25.5×10^8 yeast cells were harvested by centrifugation (4000 rpm, 5 min, 30 °C). The pellet was suspended in 15 ml growth medium containing 50 μg/ml cycloheximide (Sigma–Aldrich) for 5 min at 30 °C, and 35 ml ice-cold water was added. After centrifugation (4000 rpm, 5 min, 4 °C), cells were suspended in 600 μl lysis buffer (10 mM Tris–HCl, pH 7.5, 100 mM NaCl, 30 mM $MgCl_2$, and 50 μg/ml cycloheximide) and incubated for 5 min on ice. Glass beads (200 μl; Sigma–Aldrich) were added and the cells were lysed by vortexing (four times, 1 min, 4 °C). The lysates were clarified by centrifugation (10,000 rpm, 10 min, 4 °C). Ten $A_{260\ nm}$ units was loaded onto a 10.5-ml linear sucrose gradient (7–47%) in 50 mM Tris–acetate, pH 7.0, 50 mM NH_4Cl, 12 mM $MgCl_2$, 1 mM dithiothreitol. Ribosomes were sedimented by centrifugation (38,000 rpm, 2 h, 4 °C) using a Beckman SW41 rotor and the polysome profile was obtained by measuring $A_{254\ nm}$ with a density gradient fractionator (Teledyne ISCO).

Analysis of protein neosynthesis rate

Yeast cells (8.5×10^7) grown under the various conditions were labeled for 4 min with 20 μCi [^{35}S]methionine (PerkinElmer) at different time points of H_2O_2 treatment. Cells were harvested, washed with 1 ml ice-cold water, and suspended in 200 μl of 20% trichloroacetic acid (TCA). Five microliters was withdrawn to measure [^{35}S]methionine incorporation into the cells. Glass beads (200 μl) were added and cells were disrupted by vortexing (two times, 1 min, 4 °C). Supernatant and washes with 5% TCA were combined before centrifugation (3000 rpm, 10 min, room temperature). The protein pellet was suspended in 100 μl Laemmli buffer, boiled for 5 min, and centrifuged (3000 rpm, 10 min, room temperature). The soluble proteins were transferred into a new tube and the radioactivity of 10 μl was measured by scintillation counting. The values were normalized to the radioactivity present into the cells.

Nuclear DNA mutation frequency

The occurrence of Can^r mutation was measured as described [43], with minor modifications. For each growth condition, more than five cultures of Δ*gsh1* cells were treated with 400 μM H_2O_2 for 60 min, harvested by centrifugation, and plated onto S100 + 100 μM GSH + 0.8% agarose solid medium, to determine the total number of viable cells, and onto S100 + 100 μM GSH + 0.8% agarose solid medium containing 60 mg/L L-canavanine sulfate salt (Sigma–Aldrich), to determine the number of Can^r mutants. Plates were counted after 4 days incubation at 30 °C. The mutation frequency and the value of the 95% confidence interval were calculated using the MSS–maximum likelihood estimator method through the fluctuation analysis calculator (FALCOR) available at http://www.keshavsingh.org/protocols/FALCOR.html [44].

Results

GSH protects proteins against carbonylation under oxidative stress

To investigate the role of GSH during oxidative stress, we used two different strategies that depleted yeast cells of intracellular GSH before H_2O_2 treatment. The first strategy consisted in shifting exponentially growing WT cells from a culture medium containing 100 μM sulfate (S100) to a culture medium deprived of all sources of sulfur (S0) [25]. Under these conditions, cells strongly increase GSH degradation to use it as a source of sulfur [25]. Accordingly, intracellular concentration of total GSH dropped from nearly 1 mM to less than 0.03 mM in 60 min (Fig. 1A). The second strategy used a Δ*gsh1* strain, which is unable to synthesize GSH and requires low doses of GSH in the culture medium to grow [20]. Δ*gsh1* cells were able to grow in the absence of additional GSH for more than eight generations (8G), as already described [26,27], but with a slight increase in the doubling time (Supplementary Fig. S1). Under these conditions, the intracellular concentration of total GSH dropped from approximately 4 mM to less than 0.03 mM (Fig. 1A).

Because GSH is considered a central redox buffer [21], we investigated the consequences of GSH depletion on protein oxidation. To this purpose, we first used semiquantitative Western blot analyses to measure the amount of carbonylated proteins in total protein crude extracts [39]. Protein carbonylation signals were nearly identical in S100 and S0 crude extracts (S100/S0 = 0.92 ± 0.08; Fig. 1B, lane 1 vs 3), suggesting that GSH depletion had no impact on the carbonylation level of WT cells. The same observation was made with Δ*gsh1* cells (+GSH/8G = 1.01 ± 0.095; Fig. 1B, lane 5 vs 7). However, when cells were submitted to a mild H_2O_2 treatment (400 μM for 60 min), proteins of deprived cells (cells grown under sulfur starvation or GSH depletion) were significantly more oxidized than proteins of nondeprived cells (Fig. 1B, and quantifications). Next, we monitored the effect of GSH depletion on protein-thiol oxidation by using the redox-sensitive yellow fluorescent protein (rxYFP) [45,46]. Redox Western blot analyses revealed that protein-thiols were not affected in WT cells grown under sulfur starvation and only slightly more oxidized in 8G GSH-depleted Δ*gsh1* cells (Supplementary Fig. S2). In agreement with the protein carbonylation signal, the rxYFP probe was fully oxidized by H_2O_2 treatment in cells grown under depleted conditions (WT S0 and Δ*gsh1* 8G), whereas it remained essentially reduced in cells grown under nonstarved conditions (S100 and +GSH) (Supplementary Fig. S2). These results demonstrated that in addition to its role in preserving protein-thiols from oxidation, GSH also protects intracellular proteins against carbonylation under oxidative stress.

GSH preserves cell survival under oxidative stress

Because accumulation of carbonylated proteins has been associated with a severe decrease in cell viability [13,14], we monitored the impact of GSH depletion on the survival of H_2O_2-treated cells. When WT cells were grown in S100 medium, H_2O_2 mildly

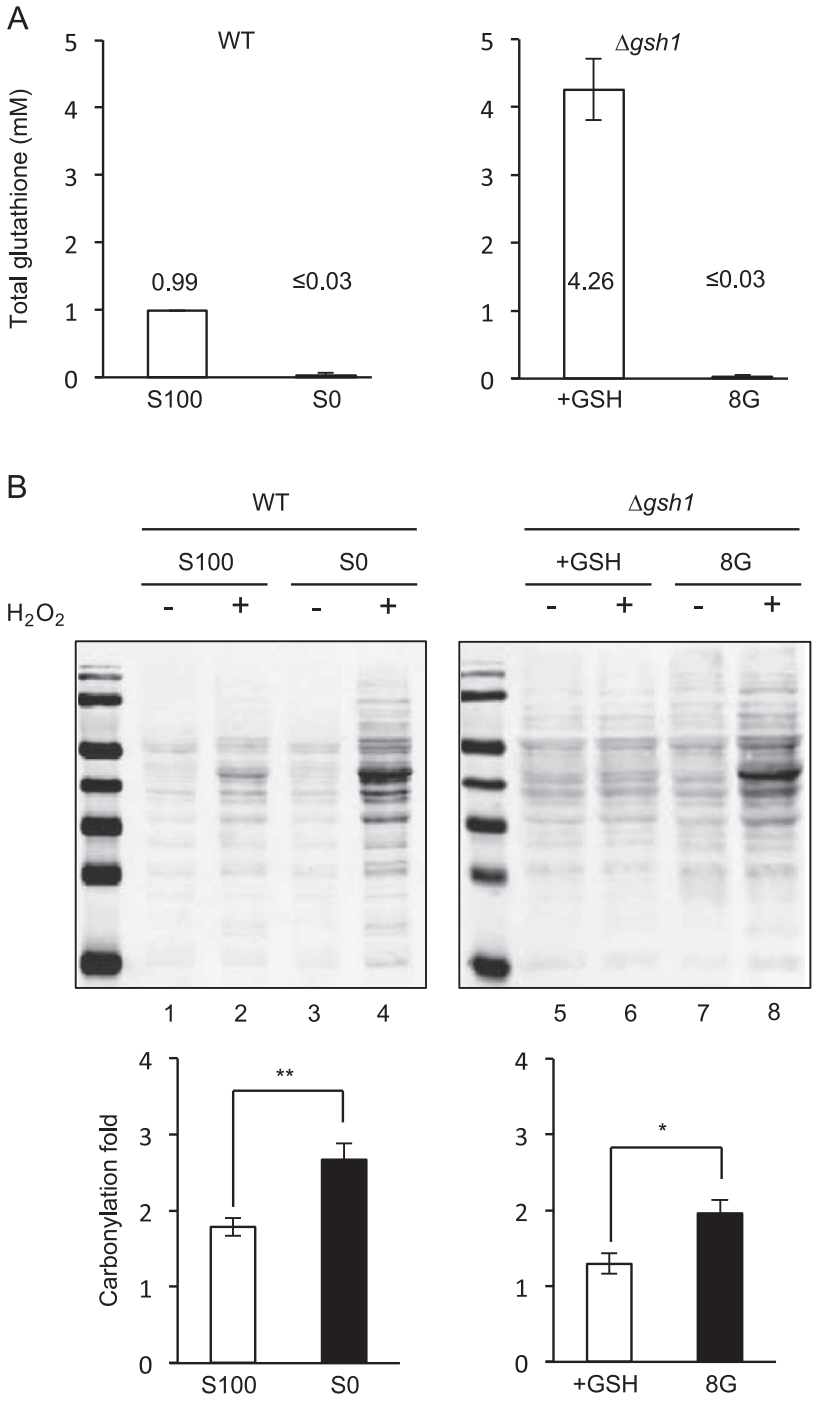

Fig. 1. GSH protects cellular proteins against carbonylation under H_2O_2 treatment. (A) The cellular content of total glutathione was measured in WT cells grown under normal conditions (S100) or after 60 min of sulfur starvation (S0) (left). For the Δ*gsh1* strain (right), cells were harvested from culture grown in S100 medium supplemented with 100 μM GSH (+GSH) or after 8 G of GSH depletion in S100 medium. Values are the mean ± standard deviation (SD) of at least three independent experiments. (B) Analysis of protein carbonylation in WT and Δ*gsh1* cells grown under normal or deprived conditions before being treated, or not, with 400 μM H_2O_2 for 60 min. Total protein crude extracts were derivatized with DNPH, and the levels of carbonylated proteins were quantified by Western blot analysis using anti-DNP antibodies. Signals were normalized to the basal carbonyl content before H_2O_2 treatment (set to 1) and plotted as fold of carbonylation. Values are the mean ± SD of at least three independent experiments. $^{*}P < 0.05$ and $^{**}P < 0.01$, Student's *t* test, compared to nondeprived conditions.

affected cell survival, which decreased to 43% after a 60-min treatment (Fig. 2A), consistent with previous reports [47,48]. But when WT cells were under sulfur starvation, H_2O_2 had a dramatic effect on the survival rate, which decreased to 1.8 and 0.1% after a 20- and 60-min treatment, respectively (Fig. 2A). Of note, growth in S0 medium did not affect the viability of WT cells (Supplementary Fig. S3A). Similar results were obtained with Δ*gsh1* cells: the survival rate of cells submitted to 60 min of 400 μM H_2O_2 dropped to 40.7%, when they were grown in presence of GSH (+GSH), and to 7.8%, when they were preliminarily GSH-depleted for 8G (Fig. 2B and Supplementary Fig. S3B). These results demonstrated that cells containing a very low concentration of GSH (< 0.03 mM) were not protected against oxidative stress, as exemplified by the high accumulation of carbonylated proteins, the complete oxidation of the rxYFP probe, and the low survival rate.

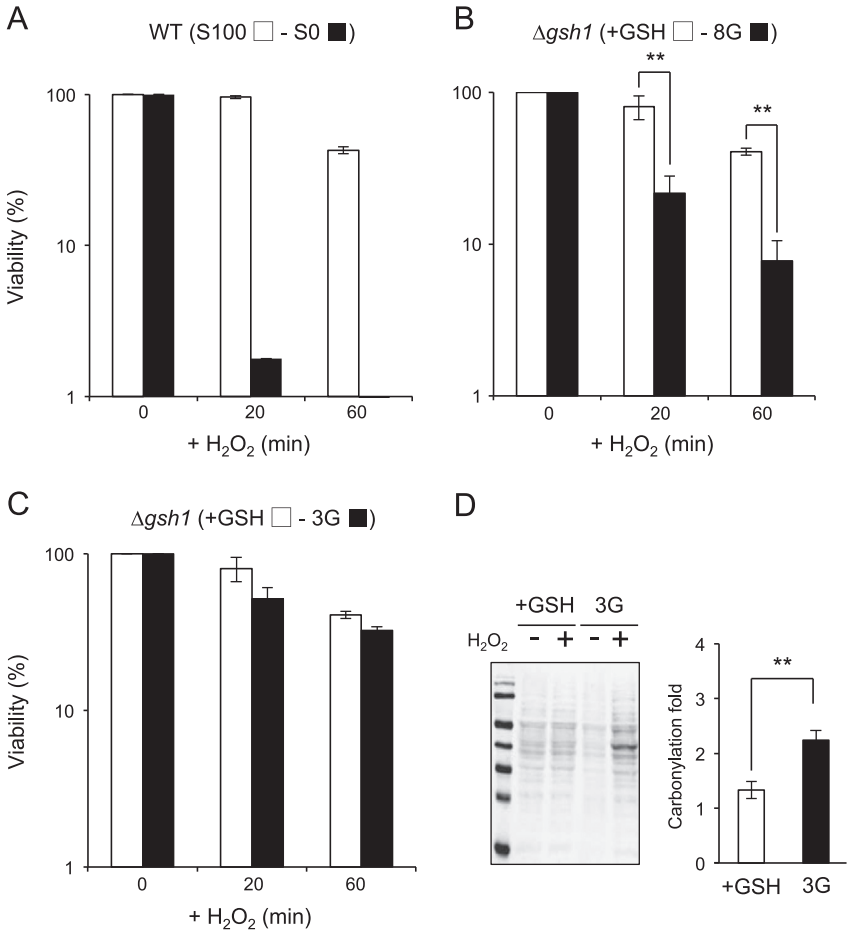

Fig. 2. GSH is essential for cell survival under H_2O_2 stress conditions. (A) To determine cell survival, WT cells were grown in S100 medium before being submitted, or not, to sulfur starvation and treated with 400 μM H_2O_2. At $t=0$, 20, and 60 min, cells were harvested and colony-forming units were determined after 3 days incubation on S100+GSH plates. Percentage of viability was calculated compared to viability at $t=0$ (set to 100%). Values are the mean ± SD of at least three independent experiments. (B) Same experiment as in (A) with Δ*gsh1* cells grown in S100+GSH medium or after 8 G of GSH depletion in S100 medium. $^{**}P<0.01$, Student's *t* test, compared to nondepleted conditions. (C) Same experiment as in (A) except that Δ*gsh1* cells were grown in the absence of GSH for 3G. (D) The level of carbonylated proteins in Δ*gsh1* cells grown under normal conditions (+GSH) or in the absence of GSH for 3G before being treated, or not, with 400 μM H_2O_2 for 60 min was assessed as in Fig. 1B. Values are the mean ± SD of at least three independent experiments. $^{**}P<0.01$, Student's *t* test, compared to nondepleted conditions.

To identify the minimal concentration of GSH required to preserve cell viability, we grew Δ*gsh1* cells in a culture medium without GSH for different amounts of time before treating them with H_2O_2. Analysis of cell survival revealed that three generations (3G) of GSH depletion had no significant impact on cell viability under H_2O_2 treatment (Fig. 2C). Under these conditions, the intracellular concentration of total GSH dropped to 0.08 mM ± 0.023. However, Western blot analyses revealed that proteins of 3G-depleted cells were highly sensitive to H_2O_2 treatment, as shown by the accumulation of carbonylated proteins (Fig. 2D) and the redox profile of the rxYFP probe (Supplementary Fig. S2). We concluded that a low concentration of intracellular GSH (0.08 mM) is sufficient to preserve cell viability under oxidative stress and that accumulation of carbonylated proteins does not systematically correlate with cell mortality.

GSH-depleted cells are not preadapted to oxidative stress conditions

We wondered whether the higher viability of Δ*gsh1* cells during H_2O_2 treatment, compared to WT cells (7.8% vs 0.1%, see above), could be due to cell adaption to depleted conditions. Indeed, 60 min of sulfur starvation may not be sufficient for WT cells to set up an adaptive response to oxidative stress, whereas GSH depletion of Δ*gsh1* cells for more than 16 h (8G) could lead to the induction of enzymes involved in the oxidative stress response. To evaluate this hypothesis, we first analyzed protein neosynthesis in WT cells grown under S0 conditions and in 3G and 8G GSH-depleted Δ*gsh1* cells. The proteomes were radiolabeled with [^{35}S]methionine and compared by two-dimensional gel electrophoresis [49]. Overall analyses of radioactive labeling and Coomassie blue staining showed that protein neosynthesis and protein abundance were very similar in deprived and nondeprived cells (Supplementary Figs. S4 and S5). However, spot-by-spot analysis revealed that, as expected [50], WT cells grown under sulfur starvation displayed an increased synthesis of proteins involved in the yeast sulfur metabolism (Supplementary Fig. S4). This induction was not observed in Δ*gsh1* cells grown under GSH-depleted conditions. Nevertheless, these cells showed a very faint accumulation of oxidized Tsa1 (Supplementary Fig. S5), but surprisingly none of the other proteins accumulated in their oxidized form. This observation confirmed that, as suggested by the mild oxidation of the rxYFP probe, some protein-thiols might be slightly oxidized by the GSH depletion in Δ*gsh1* cells.

Finally, we performed RT-PCR analysis and confirmed that oxidative stress-responsive genes were not (*CCP1* and *CTT1*) or were only poorly (*TRX2*) induced in Δ*gsh1* cells during GSH depletion (Supplementary Fig. S6A). We also showed that catalase

activity of GSH-depleted Δ*gsh1* cells remained at the same low level as catalase activity of Δ*gsh1* cells grown in the presence of GSH (Supplementary Fig. S6B). We concluded from these experiments that the survival rate of H_2O_2-treated Δ*gsh1* cells was not due to the induction of oxidative stress-responsive proteins during GSH depletion.

GSH depletion increases the labile iron pool and impedes H_2O_2 degradation machineries

Protein carbonylation is mostly due to hydroxyl radicals produced through the Fenton reaction from iron and H_2O_2 [7]. Upon exposure to H_2O_2, the increase in carbonylated proteins measured in GSH-depleted cells could thus be attributed to an increase in intracellular iron and/or an increase in intracellular H_2O_2. As shown in Fig. 3A, the whole-cell iron concentration of WT and Δ*gsh1* cells remained constant, whatever the growth conditions. This result was unexpected, as previous reports described an accumulation of iron in Δ*gsh1* cells grown under GSH depletion in SD minimal medium (SD-MM) [29]. Accordingly, we observed that intracellular iron concentration increased with GSH depletion when cells were grown in SD-MM (Fig. 3A), suggesting that iron accumulation under GSH depletion is dependent upon the composition of the growing medium. These observations were confirmed by the very poor induction of *FET3* transcription in S100 medium (Fig. 3B), a typical gene controlled by Aft1, the transcription factor that regulates iron uptake [51]. Disruption of iron homeostasis in GSH-depleted Δ*gsh1* cells is also considered to be responsible for mitochondrial genome instability, leading to the irreversible loss of respiratory competency [29]. We thus assessed the respiratory competency of Δ*gsh1* cells grown in the presence of GSH or under 3G and 8G GSH-depleted conditions. We observed that the proportion of respiratory incompetent cells remained almost constant, whatever the growth conditions (Supplementary Fig. S7). Altogether, these results demonstrated that WT cells grown under sulfur starvation and Δ*gsh1* cells grown under GSH depletion did not initiate an iron starvation-like response. Alternatively, it was possible that GSH depletion led to an increase in the labile iron pool, which could be released from inactivated Fe/S-containing enzymes [34]. We addressed this question by monitoring the fluorescence of calcein, a metal-sensitive probe whose fluorescence decreases when it binds to the labile iron pool [34]. As shown in Fig. 3C, calcein fluorescence was significantly lower in GSH-depleted Δ*gsh1* cells (3G and 8G) than in +GSH Δ*gsh1* cells, indicating an increase in the labile iron pool in GSH-depleted Δ*gsh1* cells. This variation of the labile iron pool could explain the accumulation of carbonylated proteins in GSH-depleted Δ*gsh1* cells submitted to H_2O_2 treatment, because it might become available to promote the Fenton reaction.

Nevertheless, the high level of carbonylated proteins measured in cells grown under GSH depletion could also be due to the accumulation of intracellular H_2O_2. Because all cultures received the same initial amount of H_2O_2, this hypothesis implied that GSH depletion would impair H_2O_2 detoxification machineries and, as a consequence, H_2O_2 degradation capacity. To address this question, we monitored the evolution of H_2O_2 concentration in the supernatant of H_2O_2-treated cultures. We observed that the degradation rate of H_2O_2 was significantly higher in WT cells grown under the S100 condition compared to WT cells grown under sulfur starvation (Fig. 4). Similarly, we observed a higher degradation rate of H_2O_2 in Δ*gsh1* cells grown in the presence of GSH, compared to cells grown under 3G and 8G GSH depletion (Fig. 4). We concluded that sulfur starvation and GSH depletion affected the efficiency of H_2O_2 detoxification machineries under oxidative stress conditions, suggesting that the accumulation of carbonylated proteins in cells

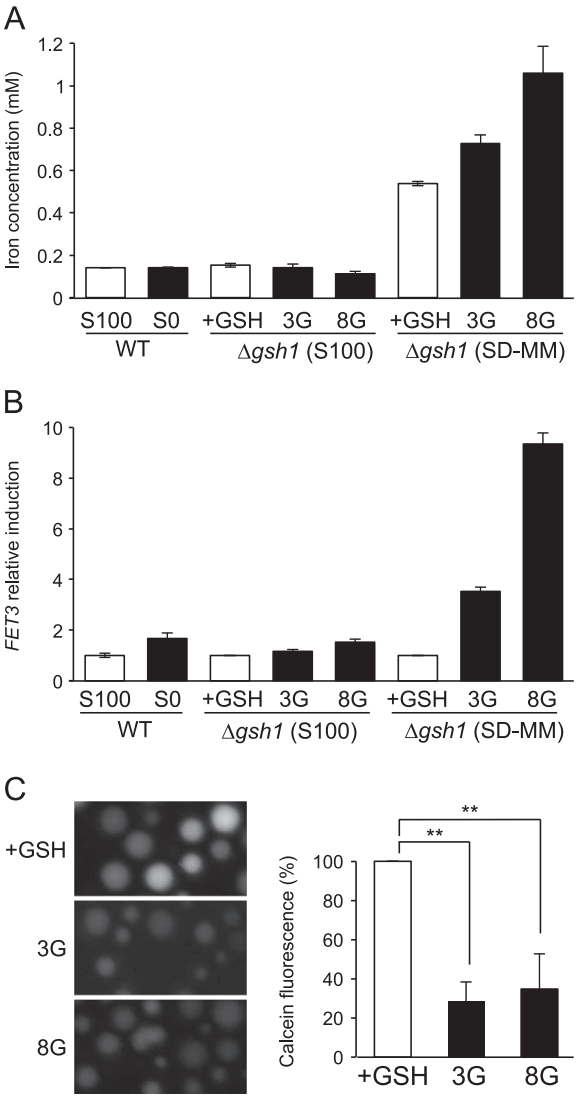

Fig. 3. Sulfur starvation and GSH depletion do not affect iron homeostasis but impair H_2O_2 degradation. (A) Dosage of whole-cell iron concentration in WT and Δ*gsh1* cells grown under normal conditions (S100 or +GSH, white bars) or under deprived conditions (sulfur starvation (S0) or GSH depletion for 3G and 8G, black bars). The same experiment was performed with Δ*gsh1* cells grown in SD minimal medium (SD-MM). Values are the mean ± SD of at least three independent experiments. (B) WT and Δ*gsh1* cells were grown as in (A). Total RNAs were extracted and *FET3* and *ACT1* mRNAs were quantified by RT-PCR. *FET3* expression was normalized to *ACT1* and the ratio to the corresponding nondeprived condition is represented. Values are the mean ± SD of two independent experiments, each experiment analyzed in triplicate. (C) Δ*gsh1* cells were grown as in (A) and 5 μM calcein was added to the cultures. After 2 h of incubation, the calcein fluorescence was assessed by fluorescence microscopy (see Materials and methods). The fluorescence signal was measured by image quantification and represented as a percentage of the signal measured in Δ*gsh1* cells grown in S100+GSH (set to 100%). Values are the mean ± SD of four independent experiments. $^{**}P < 0.01$, Student's *t* test, compared to nondeprived conditions.

grown under depleted conditions results from both an increase in the labile iron pool and a decrease in H_2O_2 degradation capacity.

Only high GSH concentrations preserve translational activity during oxidative stress

Because we demonstrated that sulfur starvation and GSH depletion did not induce an oxidative stress response before H_2O_2 treatment, the defect of H_2O_2 detoxification in deprived cells was probably due to either a dysfunction in the induction of

stress-responsive proteins or an impairment of the activity of H_2O_2 detoxifying enzymes.

To assess protein neosynthesis in H_2O_2-treated cells, we monitored the evolution of [^{35}S]methionine incorporation into proteins. As previously reported [1,52], we observed that in the absence of deprivation, WT and Δ*gsh1* cell translational activities were inhibited by oxidative stress (Fig. 5A). Indeed, the translational activity of WT cells was totally abolished before being restored, after 30 min of H_2O_2 treatment, to 18% of the initial activity; and the translational activity of Δ*gsh1* cells decreased to reach a plateau at 28.5% of the initial activity. Under all other conditions, incorporation of [^{35}S]methionine into proteins was close to zero (Fig. 5A). This suggested that the translational activity of WT cells grown under sulfur starvation, and of GSH-depleted Δ*gsh1* cells, was abolished by oxidative stress.

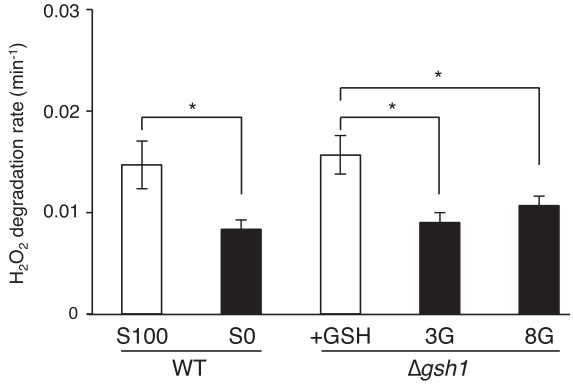

Fig. 4. WT and Δ*gsh1* cells were grown under normal conditions (S100 or +GSH, white bars) or under deprived conditions (sulfur starvation (S0) or GSH depletion for 3G and 8G, black bars) and 400 μM H_2O_2 was added to induce oxidative stress. H_2O_2 remaining in the culture medium was measured at different time points during 60 min and the H_2O_2 degradation rates were deduced from exponential fitting of the curves (see Materials and methods). Values are the mean ± SD of at least three independent experiments. $^*P < 0.05$, Student's *t* test, compared to nondeprived conditions.

To confirm these results, we performed polysome profiling [1]. When WT and Δ*gsh1* cells were grown under normal conditions (WT S100 and Δ*gsh1* +GSH), we observed that oxidative stress led to a small decrease in polysomal peaks and to an increase in the 80S peak (Fig. 5B), reflecting a global downregulation of translational activity [1]. When WT cells were grown under sulfur starvation, oxidative stress had a dramatic impact: polysomal peaks disappeared in favor of the 80S peak (Fig. 5B). We observed the same phenomenon, to a lower extent, for 3G and 8G GSH-depleted Δ*gsh1* cells (Fig. 5B), thus confirming that GSH depletion of Δ*gsh1* cells led also to the shutdown of protein synthesis during oxidative stress.

Altogether, our observations demonstrated that a high concentration of GSH was required to maintain the global translational activity of H_2O_2-treated cells. These results explained the low efficiency of H_2O_2 degradation machineries in deprived cells. Furthermore, because the 3G GSH-depleted Δ*gsh1* cells had the

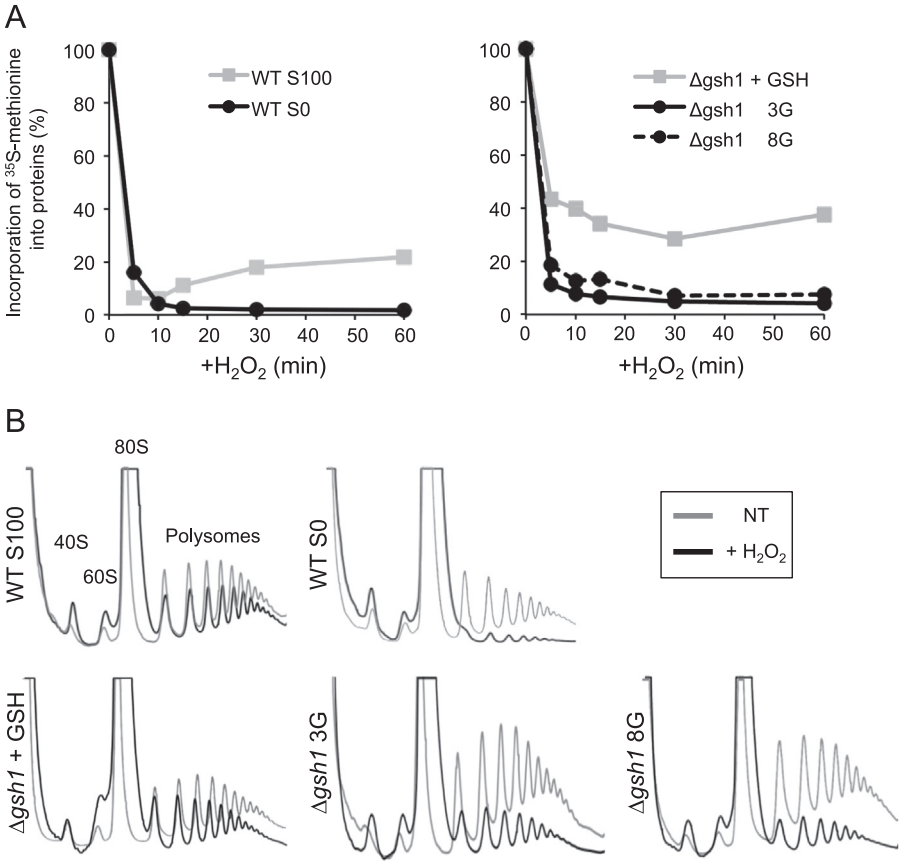

Fig. 5. GSH is required for protein synthesis during oxidative stress. (A) Protein neosynthesis was measured by [^{35}S]methionine pulse labeling. WT and Δ*gsh1* cells were grown under normal or deprived conditions before being treated with 400 μM H_2O_2. At different time points of H_2O_2 treatment, cells were incubated with [^{35}S]methionine for 4 min before being harvested. [^{35}S]Methionine incorporation into the cells and into proteins was measured by liquid scintillation. The signal from radioactive proteins was normalized to the rate of [^{35}S]methionine incorporated into the cells and represented as a percentage of incorporation in absence of treatment ($t=0$, set to 100%). (B) WT and Δ*gsh1* cell translational activities were assessed by polysome profiling. Cells were grown under normal or deprived conditions before being treated or not with 400 μM H_2O_2 for 60 min. Cells were harvested in the presence of cycloheximide and ribosomal particles were separated on sucrose gradient from total lysate. The polysome profile was obtained by measuring the A_{254nm} of fractions collected from the gradient. Peaks of 40S and 60S ribosomal subunits as well as 80S ribosomes are indicated. The polyribosome peaks are also marked.

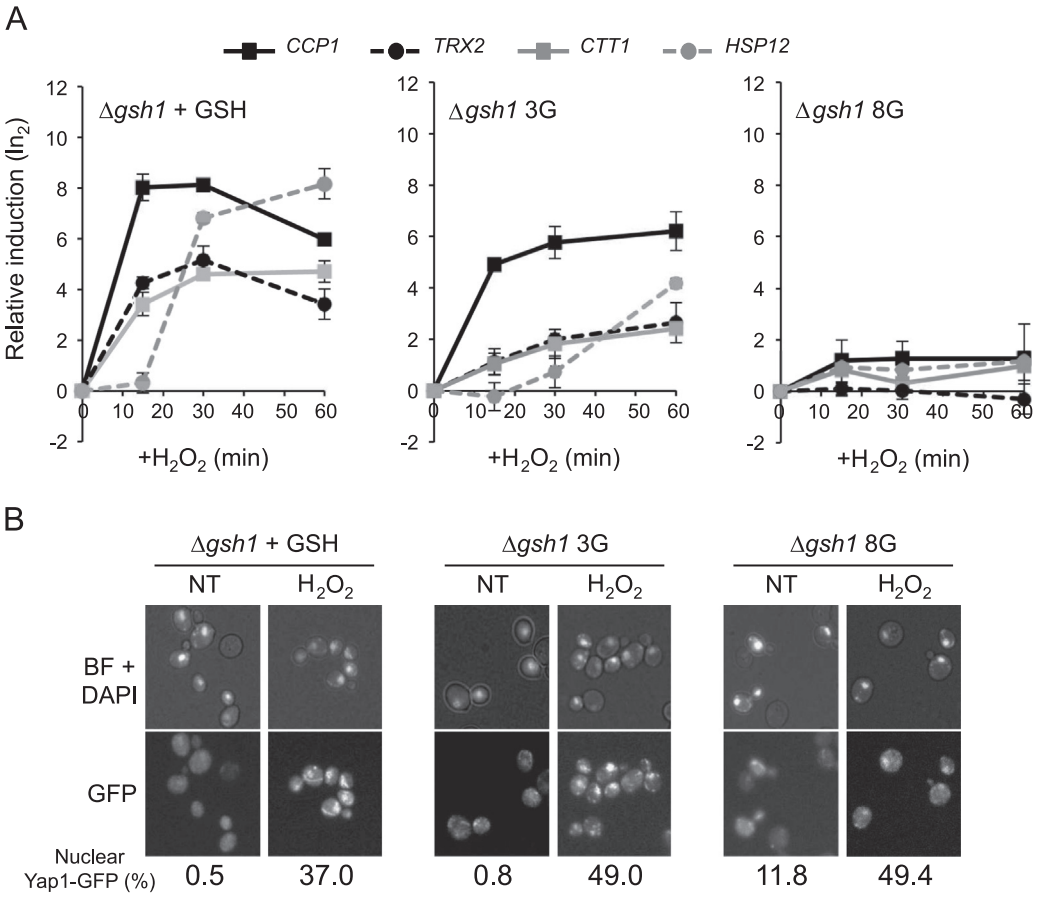

Fig. 6. GSH depletion affects gene transcription but does not alter Yap1 nuclear accumulation in response to H_2O_2 treatment. (A) Transcriptional induction of Yap1-controlled genes (*CCP1* and *TRX2*) and Msn2-controlled genes (*CTT1* and *HSP12*) was monitored by RT-PCR. Δ*gsh1* cells were grown in S100 medium under normal conditions (+GSH) or under GSH depletion for 3G or 8G. Cells were harvested after 0, 15, 30, and 60 min of the subsequent H_2O_2 treatment (400 μM). Total mRNAs were extracted and the expression of *CCP1, TRX2, CTT1,* and *HSP12* was quantified by RT-PCR. Ln_2 of induction fold compared to $t=0$ (set to 0) was calculated after normalization to *ACT1* signals. Values are the mean ± SD of two independent experiments, each experiment analyzed in triplicate. (B) Yap1 nuclear accumulation was monitored in Δ*gsh1* cells carrying a Yap1–GFP fusion protein. Cells were grown in S100 medium under normal conditions (+GSH) or under GSH depletion for 3G or 8G before being treated, or not (NT), with 400 μM H_2O_2 for 30 min. Cells were harvested, nuclei were DAPI-stained, and Yap1–GFP localization was assessed by fluorescence microscopy. Percentage of cells displaying a Yap1–GFP nuclear accumulation is indicated. Values are the mean of three independent experiments. BF, bright field.

same survival rate as GSH-replete cells, we concluded that the maintenance of the cellular translational activity during mild oxidative stress was not essential to preserve cell viability.

A minimal concentration of GSH is essential to maintain the transcriptional response to oxidative stress

Oxidative modifications of cytosolic proteins, in particular carbonylation of the translational machinery [53], were likely to be responsible for the lack of translational activity in H_2O_2-treated cells grown under deprivation. However, this lack could also be due to an inhibition of the transcriptional response in GSH-depleted cells. To test this hypothesis, we measured the induction of stress-responsive genes by RT-PCR. We focused our analyses on genes that are highly induced in response to oxidative conditions, such as those controlled by the Yap1 transcription factor (e.g., *CCP1* and *TRX2* [17]) and those controlled by the Msn2 transcription factor (e.g., *CTT1* and *HSP12* [47]). As expected, the transcriptional response of Δ*gsh1* cells grown in the presence of GSH was fully efficient (Fig. 6A). In contrast, gene induction of 8G GSH-depleted Δ*gsh1* cells was severely impaired (Fig. 6A). We obtained the same results for WT cells grown in S0 medium (Supplementary Fig. S8A). The RT-PCR experiments also revealed that although some attenuation and delay could be noticed, the transcriptional activation of stress-responsive genes was not markedly affected in 3G GSH-depleted cells (Fig. 6A). We concluded that a minimal concentration of GSH, such as 0.08 mM (3G condition), was required to preserve the transcriptional response in H_2O_2-treated cells. However, our results strongly suggested that transcriptional activity, per se, was not directly responsible for the survival of 3G GSH-depleted Δ*gsh1* cells, as the strong inhibition of the translational machinery made the translation of mRNAs into proteins impossible. In this context, the transcriptional response observed in 3G GSH-depleted Δ*gsh1* cells could simply reflect the fact that a low concentration of GSH (such as 0.08 mM) was essential to preserve nuclear function.

Because the nuclear accumulation of stress-responsive transcription factors is considered to be the first step in the transcriptional response, we analyzed the nuclear accumulation of a Yap1–GFP fusion protein expressed in Δ*gsh1* cells. Fluorescence microscopy showed an efficient nuclear accumulation of Yap1–GFP both in Δ*gsh1* (Fig. 6B) and in WT (Supplementary Fig. S8B) cells, independent of the growth conditions. Thus, under a very low concentration of intracellular GSH (< 0.03 mM), the cell transcriptional activity was inhibited, despite the proper nuclear accumulation of the dedicated transcription factor.

GSH is required to preserve nuclear DNA and nuclear function during oxidative stress

Nuclear oxidation has many deleterious consequences. In particular, it causes DNA damage, leading to a broad spectrum of mutations [43]. To study the consequences of GSH depletion on

H_2O_2-induced DNA damage, we monitored the nuclear genome stability by using a Can^r mutation assay [46]. In the absence of H_2O_2 treatment, the stability of the nuclear genome of Δ*gsh1* cells was not affected by any of the depleting conditions (mutation frequency $< 1.0 \times 10^{-7}$, Fig. 7A). When H_2O_2 treatment was applied on Δ*gsh1* cells grown in the presence of GSH or after 3G of GSH depletion, we observed a mild increase in the mutation frequency, which reached 3.3×10^{-7} and 7×10^{-7} (Fig. 7A). But when Δ*gsh1* cells were GSH-depleted for 8G, mutation frequency increased to 17×10^{-7}, showing that nuclear DNA stability is strongly affected by H_2O_2 treatment under very low GSH concentrations. Genome instability measured with the Can^r assay is a result of a balance between the presence of DNA-damaging agents and the DNA repair processes. As Rad53 is an essential checkpoint kinase that is a key player in the DNA damage response [54,55], we used Western blot analyses to investigate its activation (i.e., phosphorylation [56]) in Δ*gsh1* cells. As shown in Fig. 7B, H_2O_2 treatment induced a slight Rad53 phosphorylation in Δ*gsh1* cells grown in the presence of GSH, whereas Rad53 phosphorylation was marked in 3G GSH-depleted cells. But strikingly, Rad53 activation was totally abolished in 8G GSH-depleted Δ*gsh1* cells (Fig. 7B). This result suggested that under very low GSH concentration (< 0.03 mM), essential nuclear activities, such as transcription and DNA damage signaling, were impaired during H_2O_2 treatment. To assess the specificity of this inhibition, we performed the same experiment but replaced the oxidative stress by a treatment with hydroxyurea (HU), a drug that inhibits DNA replication and activates Rad53 [56,57]. We observed that Rad53 was markedly activated by HU treatment, demonstrating that Rad53 activation was still efficient under very low concentrations of GSH and that Rad53 inhibition was specific to H_2O_2 treatment under GSH depletion.

Altogether, these results showed that nuclear components of GSH-depleted cells were highly sensitive to oxidative damage. This suggested that nuclear proteins of GSH-depleted Δ*gsh1* cells could also be prone to carbonylation. To test this hypothesis, we monitored the carbonylation of histones purified from Δ*gsh1* cells grown under the various conditions, before or after being submitted to H_2O_2 treatment. Similar to the mutation frequency data, semiquantitative Western blot analyses showed that histones of 8G GSH-depleted Δ*gsh1* cells were highly carbonylated under oxidative stress (Fig. 7C), whereas the carbonylation level of histones from both of the other growth conditions remained significantly lower. We concluded that nuclei of 8G GSH-depleted Δ*gsh1* cells were highly oxidized during H_2O_2 treatment, demonstrating that GSH had an essential role in preserving nuclear function from deleterious oxidative modifications.

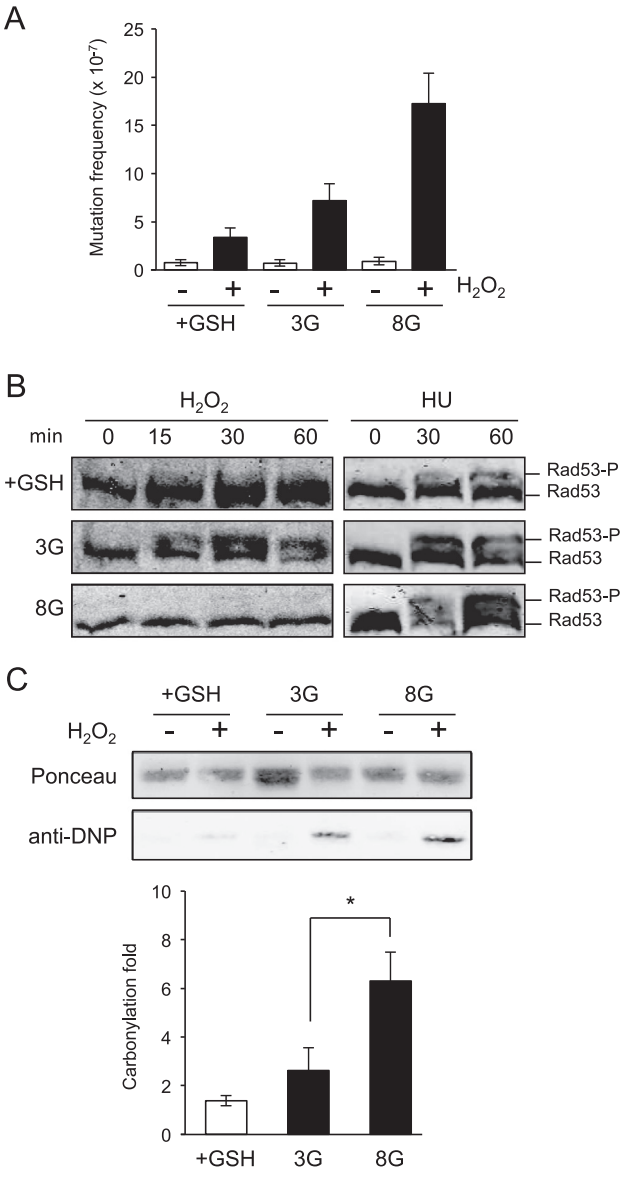

Fig. 7. GSH is required to preserve nuclear function during oxidative stress. (A) H_2O_2-induced DNA mutations were assessed using the Can^r assay [43]. Δ*gsh1* cells were grown in S100 medium under normal conditions (+GSH) or under GSH depletion for 3G or 8G. They were submitted (black bars), or not (white bars), to oxidative stress for 60 min and were plated on solid medium with or without 60 mg/L of L-canavanine. After 3 days of growth at 30 °C, colony-forming units were determined and the Can^r mutation frequency was calculated as described under Materials and methods. The 95% confidence interval values are indicated (error bars). (B) Rad53 phosphorylation pattern was analyzed in Δ*gsh1* cells grown in S100 medium under normal conditions (+GSH) or under GSH depletion for 3G or 8G. Cells were treated with either 400 μM H_2O_2 or 0.2 M HU and harvested at different time points. Protein crude extracts were prepared and Rad53 phosphorylation pattern was revealed by Western blot analysis. Positions of the bands corresponding to nonphosphorylated (Rad53) and phosphorylated (Rad53-P) forms of Rad53 are indicated. (C) Δ*gsh1* cells were grown in S100 medium under normal conditions (+GSH) or under GSH depletion for 3G or 8G. They were treated, or not, with 400 μM H_2O_2 for 60 min and histone purification was performed as described under Materials and methods. Pure histones were derivatized with DNPH, and the levels of carbonylated histones were quantified by Western blot analysis using anti-DNP antibodies. The signals were normalized to the basal carbonyl content (before H_2O_2 treatment, set to 1) and plotted as fold of carbonylation. Values are the mean ± SD of at least three independent experiments. *$P < 0.05$, Student's *t* test, 3G GSH depletion compared to 8G condition.

Discussion

Although GSH is known as the major redox buffer of the cell [20–22], several reports suggested that the essential role of GSH is not to protect the cells against ROS produced endogenously [26,27,29,30]. In agreement with these studies, we observed that a decrease in intracellular GSH concentration had a weak impact on cell physiology when cells were not submitted to exogenous oxidative stress. Moreover, our results confirmed that only a very low intracellular concentration of GSH was required to allow normal cell growth. We also found that the iron starvation-like response previously described in GSH-depleted cells [29,30] was dependent upon the composition of the growth medium. Indeed, under our growth conditions, we observed an increase in the labile iron pool, but we did not find evidence of an accumulation of the intracellular iron or an activation of Aft1-controlled genes (Fig. 3). Moreover, GSH depletion of Δ*gsh1* cells grown in S100 medium did not increase the frequency of respiratory-incompetent cells (Supplementary Fig. S7). Thus, the S100 growth medium was particularly adapted to study the consequences of GSH depletion,

because it did not generate other cellular stress that would be evidenced by an iron starvation-like response.

Repression of translational activity is a common feature of many stress conditions [58]. In the context of a global downregulation of protein synthesis, induction of specific proteins leads to rapid and selective changes in protein levels [58,59]. This phenomenon is an important aspect of proteome plasticity and allows a rapid response to environmental changes. As previously reported [1,3], we showed that when WT or Δ*gsh1* cells were grown under nondeprived conditions, H_2O_2 treatment led to a strong decrease in translational activity. Former studies have demonstrated that this inhibition is mainly controlled at the initiation level of translation and is regulated by the Gcn2-mediated phosphorylation of eIF2α, the α subunit of the eukaryotic initiation factor 2 (for review, see [60]). This translational downregulation was only transitory, because the translational activity resumed to a significant level after several minutes of H_2O_2 treatment. The precise characterization of 3G GSH-depleted Δ*gsh1* cells revealed unexpected results: these cells had the same survival rate as Δ*gsh1* cells grown in the presence of GSH (Fig. 2C), but displayed a complete inhibition of their translational activity upon H_2O_2 treatment (Fig. 5). Thus, synthesis of stress-responsive proteins is not a key parameter for the maintenance of cell viability during mild H_2O_2 treatment. In a previous work, we characterized a thermosensitive mutant strain containing a deletion of *RPB4*, a gene encoding an RNA polymerase II subunit [61]. Incubation of Δ*rpb4* cells at restrictive temperature led to the inhibition of mRNA synthesis and, thus, to a strong decrease in the translation of stress-responsive proteins during H_2O_2 treatment. Interestingly, we observed that WT and Δ*rpb4* cells had the same survival rate upon H_2O_2 treatment. More recently, Fomenko et al. [62] showed that a yeast strain in which the genes encoding the eight thiol-peroxidases have all been deleted is unable to activate or repress gene expression in response to H_2O_2. Again, viability of this mutant strain was not affected by a mild H_2O_2 treatment. Altogether, these observations demonstrate that the induction of stress-responsive proteins is not required to maintain cell viability under mild H_2O_2 treatment, strongly suggesting that the H_2O_2 detoxification machinery present in the cells before H_2O_2 treatment is sufficient to sustain cell viability.

Under oxidative stress, 3G GSH-depleted Δ*gsh1* cells display the same cytosolic characteristics as WT cells grown under sulfur starvation and 8G GSH-depleted Δ*gsh1* cells: proteins are highly oxidized (Fig. 2D), translational activity is impaired (Fig. 5), and H_2O_2 degradation rate is low (Fig. 4). In contrast, 3G GSH-depleted Δ*gsh1* cells display the same nuclear characteristics as GSH-replete cells, as exemplified by the transcriptional induction of stress-responsive genes (Fig. 6A), the low DNA mutation frequency (Fig. 7A), the Rad53 activation (Fig. 7B), and the moderate carbonylation of histones (Fig. 7C). Altogether, these observations demonstrate that a minimal GSH concentration is essential to protect the nucleus against oxidative damage and that maintaining nuclear function during mild H_2O_2 treatment is the key parameter of cell survival. As summarized in Fig. 8, when GSH concentration is high (> 1 mM), all cell functions are preserved from oxidative inhibition. As a result, enzymes of the detoxification machinery are induced after Yap1 nuclear accumulation, and intracellular H_2O_2 is rapidly degraded. At a lower concentration (around 0.1 mM), GSH loses its cytosolic protective effect but is still efficient for the protection of the nucleus against oxidative damage. Despite the transcriptional induction of stress-responsive genes, the detoxification machinery remains at a low level, because of the inhibition of translation. Therefore, H_2O_2 is slowly degraded and oxidized proteins accumulate in the cytosol. But upon stress release, the functional nucleus can support growth resumption. When GSH concentration drops under 0.03 mM, both nuclear and cytosolic components become highly sensitive to oxidative damage, leading to cell death. Our results highlight an apparent difference between eukaryotic and prokaryotic cells, as it was proposed that accumulation of carbonylated proteins is quantitatively related to low survival of irradiated bacteria [14,63]. But as our results showed that oxidative inhibition of cytosolic proteins is not deleterious to cell survival, only nuclear oxidation should be taken into account for the prediction of cell death during oxidative stress. The low survival of 8G GSH-depleted Δ*gsh1* cells during H_2O_2 treatment correlates with the accumulation of nuclear carbonylated proteins, as suggested by the high level of carbonylated histones (Fig. 7C). In contrast, the moderate carbonylation of nuclear proteins in 3G GSH-depleted Δ*gsh1* cells does not impede cell viability, despite high levels of cytosolic oxidized proteins. In this context, we propose that cytosolic proteins are part of a protective machinery that shields the nucleus by scavenging ROS before they can cross the nuclear membrane.

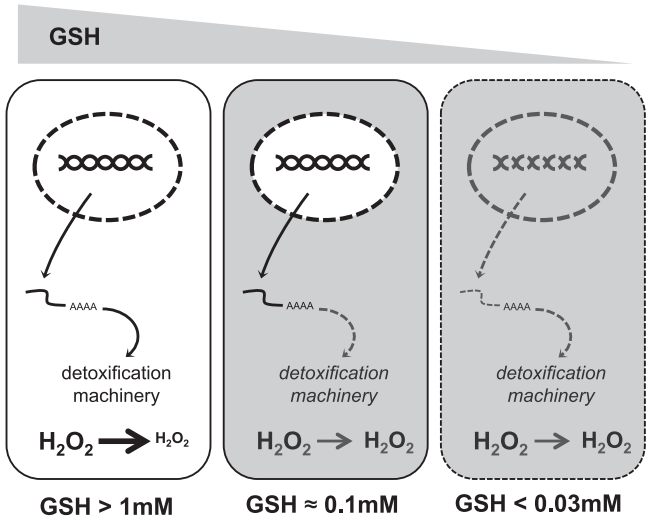

Fig. 8. GSH is essential for maintaining the nuclear function during mild H_2O_2 treatment. Under high GSH concentration (> 1 mM), both cytosolic and nuclear functions are preserved from oxidative damage, leading to high survival rates (left). A 10-fold decrease in intracellular GSH concentration (≈ 0.1 mM) still protects the nucleus against oxidative damage, but the cytosolic function is severely impaired. In absence of induction of the H_2O_2 detoxification machinery, nuclear activity is sufficient to maintain cell viability and to support growth resumption once the oxidative stress is released (middle). Under lower GSH concentration (< 0.03 mM), all cell functions are damaged by mild H_2O_2 stress conditions, thus leading to high mortality (right).

It remains to understand how GSH preserves the nucleus against lethal oxidative modifications. A first hypothesis is that under 3G GSH-depleted conditions, GSH still acts as a ROS-scavenging antioxidant in the cell nucleus, protecting proteins and DNA. Interestingly, Ayer et al. [29] found that the cytosol is more severely and rapidly affected by GSH depletion than the mitochondrial matrix and the intermembrane space. Consistently, several studies in animal and plant cells provide evidence for the existence of functionally distinct nuclear pools of GSH/GSSG that are dynamically regulated during the cell cycle [64–66]. Furthermore, studies on 3T3 fibroblasts have shown that addition of L-buthionine sulfoximine (BSO), the γ-glutamylcysteine synthetase inhibitor, significantly decreases the total cellular GSH pool, whereas the nuclear GSH pool is much more resistant than the cytosolic pool to BSO-mediated depletion [67]. In line with these observations, one can imagine that under depleted conditions, salvage mechanisms lead to a general accumulation of GSH in subcellular compartments such as the nucleus and the mitochondria. Two GSH transporters have been identified in yeast: the high-affinity GSH transporter Hgt1 [68,69] and the yeast cadmium factor 1 Ycf1 [70]. But neither Hgt1 nor Ycf1 has been implicated

in GSH nuclear accumulation, and none has been specifically localized at the nuclear membrane. Thus, validation of this hypothesis will need additional studies. In particular, the development of a reliable method to investigate GSH subcellular localization, especially under low GSH concentrations, would greatly facilitate future analyses. However, our results demonstrate that protein protection needs a high concentration of GSH, on the order of 1 mM. The nuclear yeast volume has been estimated to be approximately 7% of the cell volume [71]. If most of the GSH of 3G GSH-depleted Δ*gsh1* cells concentrates into the nucleus, the nuclear concentration of GSH could reach more than 1 mM, which would be sufficient to protect nuclear proteins against oxidative damage.

The second hypothesis is that a minimal, low concentration of GSH could be required to preserve the activity of some nuclear enzymes. However, this does not necessarily imply that GSH accumulates in the nucleus of 3G GSH-depleted Δ*gsh1* cells. In favor of this hypothesis, we obtained two unexpected results suggesting that under very low GSH concentration, the cell nucleus becomes dysfunctional during oxidative stress. First, H_2O_2 stress-responsive genes are not induced in WT cells grown under sulfur starvation or in 8G GSH-depleted Δ*gsh1* cells, despite Yap1 nuclear accumulation (Fig. 6). Previous reports have already observed that nuclear accumulation of transcription factors does not systematically correlate with the transcriptional activation of their target genes. For instance, in a Δ*msn5* mutant strain, the transcription factor Msn2 accumulates in the nucleus, but transcriptional induction of Msn2-target genes remains dependent upon stress [72]. The same observation was made with the activity of the transcriptional repressor Maf1 [73]. Thus, activation of both transcriptional effectors requires additional modifications (e.g., phosphorylation) that take place in the nucleus. A similar mechanism of activation could also apply to Yap1 and could be impaired by oxidative stress in GSH-depleted cells. Our study provided a second intriguing result that concerns Rad53 activation. Under oxidative stress, Rad53 is activated through a complex process requiring a cascade of kinase activities [74]. The fact that Rad53 was not phosphorylated in 8G GSH-depleted Δ*gsh1* cells during H_2O_2 treatment, but remained fully activated under HU treatment (Fig. 7B), strongly suggests that H_2O_2 treatment also impaired activities that are required for Rad53 activation. Thus, GSH could be essential for functions that become critical during oxidative stress, such as the activation of DNA-repair and detoxification machineries. In this context, it has been shown that GSH is required for many processes of protein folding. In particular, under GSH depletion, the cytosolic iron–sulfur protein assembly (CIA) machinery might be disturbed. As CIA activity is involved in the biogenesis of nuclear iron–sulfur proteins [75], one can assume that vital nuclear activities are missing for cell survival during oxidative stress. Sorting between these two hypotheses will be an important step forward in understanding the mechanisms responsible for minimal GSH requirement during oxidative stress.

In summary, the role of GSH has been recently reassessed under normal growth conditions, raising important questions about its essential function under oxidative stress. In this study, we characterized the physiological response of H_2O_2-treated yeast cells containing different amounts of GSH. We showed that H_2O_2 treatment of GSH-depleted cells leads to an accumulation of carbonylated proteins and an inhibition of the translational activity, correlating with a dramatic decrease in cell viability. A low amount of GSH is sufficient to rescue cell viability but, surprisingly, does not protect proteins and translational activity against oxidative injuries. A more extensive characterization of cells containing minimal amounts of GSH revealed that GSH is essential to preserve nuclear DNA and nuclear function against oxidative damage, as exemplified by low mutation frequency, moderate histone carbonylation, and activation of the checkpoint kinase Rad53 and of the H_2O_2 transcriptional response. We conclude that the essential role of GSH is to shield nuclear function, allowing cell survival and growth resumption after oxidative stress release.

Acknowledgments

We thank Matthieu Benoit, who performed the first experiments on protein carbonylation. We thank Anna Polesskya and Jéremie Kropp for help with polysome profiling, Carl Mann and Marie-Claude Marsolier-Kergoat for advice on Rad53 analysis and helpful discussions, the Nuclear Regulation and Stress Team for technical assistance and chemical reagents, and Jean-Yves Thuret and Regis Courbeyrette for help with fluorescence microscopy. Elie Hatem is a recipient of Irtélis, the CEA International Ph.D. program.

Appendix A. Supplementary material

Supplementary data associated with this article can be found in the online version at http://dx.doi.org/10.1016/j.freeradbiomed.2013.10.807.

References

[1] Shenton, D.; Smirnova, J. B.; Selley, J. N.; Carroll, K.; Hubbard, S. J.; Pavitt, G. D.; Ashe, M. P.; Grant, C. M. Global translational responses to oxidative stress impact upon multiple levels of protein synthesis. *J. Biol. Chem.* **281:**29011–-29021; 2006.

[2] Murphy, M. P. How mitochondria produce reactive oxygen species. *Biochem. J.* **417:**1; 2009.

[3] Mascarenhas, C.; Edwards-Ingram, L. C.; Zeef, L.; Shenton, D.; Ashe, M. P.; Grant, C. M. Gcn4 is required for the response to peroxide stress in the yeast Saccharomyces cerevisiae. *Mol. Biol. Cell* **19:**2995–3007; 2008.

[4] Herrero, E.; Ros, J.; Bellí, G.; Cabiscol, E. Redox control and oxidative stress in yeast cells. *Biochim. Biophys. Acta* **1780:**1217–1235; 2008.

[5] Cabiscol, E.; Piulats, E.; Echave, P.; Herrero, E.; Ros, J. Oxidative stress promotes specific protein damage in Saccharomyces cerevisiae. *J. Biol. Chem.* **275:**27393–27398; 2000.

[6] Nyström, T. Role of oxidative carbonylation in protein quality control and senescence. *EMBO J* **24:**1311–1317; 2005.

[7] Møller, I. M.; Rogowska-Wrzesinska, A.; Rao, R. S. P. Protein carbonylation and metal-catalyzed protein oxidation in a cellular perspective. *J. Proteomics* **74:**2228–2242; 2011.

[8] Sorolla, M. A.; Rodríguez-Colman, M. J.; Tamarit, J.; Ortega, Z.; Lucas, J. J.; Ferrer, I.; Ros, J.; Cabiscol, E. Protein oxidation in Huntington disease affects energy production and vitamin B6 metabolism. *Free Radic. Biol. Med* **49:**612–-621; 2010.

[9] Baraibar, M. A.; Ladouce, R.; Friguet, B. Proteomic quantification and identification of carbonylated proteins upon oxidative stress and during cellular aging. *J. Proteomics* ; 2013. (in press).

[10] Levine, R. L. Carbonyl modified proteins in cellular regulation, aging, and disease. *Free Radic. Biol. Med.* **32:**790–796; 2002.

[11] Stadtman, E. R. Protein oxidation and aging. *Free Radic. Res.* **40:**1250–1258; 2006.

[12] Dalle-Donne, I.; Aldini, G.; Carini, M.; Colombo, R.; Rossi, R.; Milzani, A. Protein carbonylation, cellular dysfunction, and disease progression. *J. Cell. Mol. Med.* **10:**389–406; 2006.

[13] Daly, M. J. Death by protein damage in irradiated cells. *DNA Repair (Amsterdam)* **11:**12–21; 2012.

[14] Krisko, A.; Radman, M. Protein damage and death by radiation in Escherichia coli and Deinococcus radiodurans. *Proc. Natl. Acad. Sci. USA* **107:**14373–14377; 2010.

[15] Murphy, M. P.; Holmgren, A.; Larsson, N. -G.; Halliwell, B.; Chang, C. J.; Kalyanaraman, B.; Rhee, S. G.; Thornalley, P. J.; Partridge, L.; Gems, D.; Nyström, T.; Belousov, V.; Schumacker, P. T.; Winterbourn, C. C. Unraveling the biological roles of reactive oxygen species. *Cell Metab.* **13:**361–366; 2011.

[16] López-Mirabal, H. R.; Winther, J. R. Redox characteristics of the eukaryotic cytosol. *Biochim. Biophys. Acta* **1783:**629–640; 2008.

[17] Lee, J.; Godon, C.; Lagniel, G.; Spector, D.; Garin, J.; Labarre, J.; Yap1, Toledano M. B. and Skn7 control two specialized oxidative stress response regulons in yeast. *J. Biol. Chem* **274:**16040–16046; 1999.

[18] Boisnard, S.; Lagniel, G.; Garmendia-Torres, C.; Molin, M.; Boy-Marcotte, E.; Jacquet, M.; Toledano, M. B.; Labarre, J.; Chédin, S. H_2O_2 activates the nuclear localization of Msn2 and Maf1 through thioredoxins in Saccharomyces cerevisiae. *Eukaryotic Cell* **8:**1429–1438; 2009.

[19] Godon, C.; Lagniel, G.; Lee, J.; Buhler, J. M.; Kieffer, S.; Perrot, M.; Boucherie, H.; Toledano, M. B.; Labarre, J. The H_2O_2 stimulon in Saccharomyces cerevisiae. *J. Biol. Chem.* **273:**22480–22489; 1998.

[20] Grant, C. M.; MacIver, F. H.; Dawes, I. W. Glutathione is an essential metabolite required for resistance to oxidative stress in the yeast Saccharomyces cerevisiae. *Curr. Genet* **29:**511–515; 1996.

[21] Schafer, F. Q.; Buettner, G. R. Redox environment of the cell as viewed through the redox state of the glutathione disulfide/glutathione couple. *Free Radic. Biol. Med* **30:**1191–1212; 2001.

[22] Zhang, H.; Forman, H. J. Glutathione synthesis and its role in redox signaling. *Semin. Cell Dev. Biol.* **23:**722–728; 2012.

[23] Penninckx, M. J. An overview on glutathione in Saccharomyces versus non-conventional yeasts. *FEMS Yeast Res* **2:**295–305; 2002.

[24] Grant, C. M.; MacIver, F. H.; Dawes, I. W. Glutathione synthetase is dispensable for growth under both normal and oxidative stress conditions in the yeast Saccharomyces cerevisiae due to an accumulation of the dipeptide gamma-glutamylcysteine. *Mol. Biol. Cell* **8:**1699–1707; 1997.

[25] Baudouin-Cornu, P.; Lagniel, G.; Kumar, C.; Huang, M. -E.; Labarre, J. Glutathione degradation is a key determinant of glutathione homeostasis. *J. Biol. Chem.* **287:**4552–4561; 2012.

[26] Lee, J. C.; Straffon, M. J.; Jang, T. Y.; Higgins, V. J.; Grant, C. M.; Dawes, I. W. The essential and ancillary role of glutathione in Saccharomyces cerevisiae analysed using a grande gsh1 disruptant strain. *FEMS Yeast Res* **1:**57–65; 2001.

[27] Spector, D.; Labarre, J.; Toledano, M. B. A genetic investigation of the essential role of glutathione: mutations in the proline biosynthesis pathway are the only suppressors of glutathione auxotrophy in yeast. *J. Biol. Chem* **276:**7011–7016; 2000.

[28] Sipos, K. Maturation of cytosolic iron–sulfur proteins requires glutathione. *J. Biol. Chem.* **277:**26944–26949; 2002.

[29] Ayer, A.; Tan, S. -X.; Grant, C. M.; Meyer, A. J.; Dawes, I. W.; Perrone, G. G. The critical role of glutathione in maintenance of the mitochondrial genome. *Free Radic. Biol. Med.* **49:**1956–1968; 2010.

[30] Kumar, C.; Igbaria, A.; Autreaux, B. I. T. D. A.; Planson, A. -G. E. L.; Junot, C.; Godat, E.; Bachhawat, A. K.; Delaunay-Moisan, A. E. S.; Toledano, M. B. Glutathione revisited: a vital function in iron metabolism and ancillary role in thiol-redox control. *EMBO J.* **30:**2044–2056; 2011.

[31] Izawa, S.; Inoue, Y.; Kimura, A. Oxidative stress response in yeast: effect of glutathione on adaptation to hydrogen peroxide stress in Saccharomyces cerevisiae. *FEBS Lett* **368:**73–76; 1995.

[32] Longtine, M. S.; McKenzie, A.; Demarini, D. J.; Shah, N. G.; Wach, A.; Brachat, A.; Philippsen, P.; Pringle, J. R. Additional modules for versatile and economical PCR-based gene deletion and modification in Saccharomyces cerevisiae. *Yeast* **14:**953–961; 1998.

[33] Tamarit, J.; Irazusta, V.; Moreno-Cermeño, A.; Ros, J. Colorimetric assay for the quantitation of iron in yeast. *Anal. Biochem* **351:**149–151; 2006.

[34] Cabiscol, E. Mitochondrial Hsp60, resistance to oxidative stress, and the labile iron pool are closely connected in Saccharomyces cerevisiae. *J. Biol. Chem* **277:**44531–44538; 2002.

[35] Rahman, I.; Kode, A.; Biswas, S. K. Assay for quantitative determination of glutathione and glutathione disulfide levels using enzymatic recycling method. *Nat. Protoc* **1:**3159–3165; 2006.

[36] Antunes, F.; Cadenas, E. Estimation of H_2O_2 gradients across biomembranes. *FEBS Lett* **475:**121–126; 2000.

[37] Laferté, A.; Favry, E.; Sentenac, A.; Riva, M.; Carles, C.; Chédin, S. The transcriptional activity of RNA polymerase I is a key determinant for the level of all ribosome components. *Genes Dev* **20:**2030–2040; 2006.

[38] Pereira, Y.; Lagniel, G.; Godat, E.; Baudouin-Cornu, P.; Junot, C.; Labarre, J. Chromate causes sulfur starvation in yeast. *Toxicol. Sci.* **106:**400–412; 2008.

[39] Levine, R. L.; Williams, J. A.; Stadtman, E. R.; Shacter, E. Carbonyl assays for determination of oxidatively modified proteins. *Methods Enzymol.* **233:**346–357; 1994.

[40] Laemmli, U. K. Cleavage of structural proteins during the assembly of the head of bacteriophage T4. *Nature* **227:**680–685; 1970.

[41] Marsolier, M. C.; Roussel, P.; Leroy, C.; Mann, C. Involvement of the PP2C-like phosphatase Ptc2p in the DNA checkpoint pathways of Saccharomyces cerevisiae. *Genetics* **154:**1523–1532; 2000.

[42] Edmondson, D. G.; Smith, M. M.; Roth, S. Y. Repression domain of the yeast global repressor Tup1 interacts directly with histones H3 and H4. *Genes Dev* **10:**1247–1259; 1996.

[43] Ragu, S.; Faye, G.; Iraqui, I.; Masurel-Heneman, A.; Kolodner, R. D.; Huang, M. -E. Oxygen metabolism and reactive oxygen species cause chromosomal rearrangements and cell death. *Proc. Natl. Acad. Sci. USA* **104:**9747–9752; 2007.

[44] Hall, B. M.; Ma, C. X.; Liang, P.; Singh, K. K. Fluctuation AnaLysis CalculatOR: a web tool for the determination of mutation rate using Luria-Delbruck fluctuation analysis. *Bioinformatics* **25:**1564–1565; 2009.

[45] Østergaard, H.; Tachibana, C.; Winther, J. R. Monitoring disulfide bond formation in the eukaryotic cytosol. *J. Cell Biol* **166:**337–345; 2004.

[46] Dardalhon, M.; Kumar, C.; Iraqui, I.; Vernis, L.; Kienda, G.; Banach-Latapy, A.; He, T.; Chanet, R.; Faye, G.; Outten, C. E.; Huang, M. -E.; Redox-sensitive, Y. F. P. sensors monitor dynamic nuclear and cytosolic glutathione redox changes. *Free Radic. Biol. Med* **52:**2254–2265; 2012.

[47] Hasan, R.; Leroy, C.; Isnard, A. -D.; Labarre, J.; Boy-Marcotte, E.; Toledano, M. B. The control of the yeast H_2O_2 response by the Msn2/4 transcription factors. *Mol. Microbiol* **45:**233–241; 2002.

[48] Cyrne, L.; Antunes, F.; Sousa-Lopes, A.; Diaz-Bérrio, J.; Marinho, H. S. Glyceraldehyde-3-phosphate dehydrogenase is largely unresponsive to low regulatory levels of hydrogen peroxide in Saccharomyces cerevisiae. *BMC Biochem* **11:**49; 2010.

[49] Vido, K.; Spector, D.; Lagniel, G.; Lopez, S.; Toledano, M. B.; Labarre, J. A proteome analysis of the cadmium response in Saccharomyces cerevisiae. *J. Biol. Chem.* **276:**8469–8474; 2000.

[50] Lafaye, A.; Junot, C.; Pereira, Y.; Lagniel, G.; Tabet, J. -C.; Ezan, E.; Labarre, J. Combined proteome and metabolite-profiling analyses reveal surprising insights into yeast sulfur metabolism. *J. Biol. Chem* **280:**24723–24730; 2005.

[51] Rutherford, J. C.; Jaron, S.; Aft1p, Winge D. R. and Aft2p mediate iron-responsive gene expression in yeast through related promoter elements. *J. Biol. Chem* **278:**27636–27643; 2003.

[52] Shenton, D.; Grant, C. M. Protein S-thiolation targets glycolysis and protein synthesis in response to oxidative stress in the yeast Saccharomyces cerevisiae. *Biochem. J* **374:**513–519; 2003.

[53] Mirzaei, H.; Regnier, F. Identification of yeast oxidized proteins: chromatographic top-down approach for identification of carbonylated, fragmented and cross-linked proteins in yeast. *J. Chromatogr. A* **1141:**22–31; 2007.

[54] Branzei, D.; Foiani, M. The Rad53 signal transduction pathway: replication fork stabilization, DNA repair, and adaptation. *Exp. Cell Res.* **312:**2654–2659; 2006.

[55] Finn, K.; Lowndes, N. F.; Grenon, M. Eukaryotic DNA damage checkpoint activation in response to double-strand breaks. *Cell. Mol. Life Sci* **69:**1447–1473; 2011.

[56] Leroy, C.; Mann, C.; Marsolier, M. C. Silent repair accounts for cell cycle specificity in the signaling of oxidative DNA lesions. *EMBO J* **20:**2896–2906; 2001.

[57] Lopes, M.; Cotta-Ramusino, C.; Pellicioli, A.; Liberi, G.; Plevani, P.; Muzi-Falconi, M.; Newlon, C. S.; Foiani, M. The DNA replication checkpoint response stabilizes stalled replication forks. *Nature* **412:**557–561; 2001.

[58] Simpson, C. E.; Ashe, M. P. Adaptation to stress in yeast: to translate or not? *Biochem. Soc. Trans.* **40:**794–799; 2012.

[59] Holcik, M.; Sonenberg, N. Translational control in stress and apoptosis. *Nat. Rev. Mol. Cell Biol.* **6:**318–327; 2005.

[60] Grant, C. M. Regulation of translation by hydrogen peroxide. *Antioxid. Redox Signaling* **15:**191–203; 2011.

[61] Maillet, I.; Buhler, J. M.; Sentenac, A.; Labarre, J. Rpb4p is necessary for RNA polymerase II activity at high temperature. *J. Biol. Chem* **274:**22586–22590; 1999.

[62] Fomenko, D. E.; Koc, A.; Agisheva, N.; Jacobsen, M.; Kaya, A.; Malinouski, M.; Rutherford, J. C.; Siu, K. -L.; Jin, D. -Y.; Winge, D. R.; Gladyshev, V. N. Thiol peroxidases mediate specific genome-wide regulation of gene expression in response to hydrogen peroxide. *Proc. Natl. Acad. Sci. USA* **108:**2729–-2734; 2011.

[63] Daly, M. J.; Gaidamakova, E. K.; Matrosova, V. Y.; Vasilenko, A.; Zhai, M.; Leapman, R. D.; Lai, B.; Ravel, B.; Li, S. -M. W.; Kemner, K. M.; Fredrickson, J. K. Protein oxidation implicated as the primary determinant of bacterial radioresistance. *PLoS Biol.* **5:**e92; 2007.

[64] Bellomo, G.; Vairetti, M.; Stivala, L.; Mirabelli, F.; Richelmi, P.; Orrenius, S. Demonstration of nuclear compartmentalization of glutathione in hepatocytes. *Proc. Natl. Acad. Sci. USA* **89:**4412–4416; 1992.

[65] Pallardó, F. V.; Markovic, J.; García, J. L.; Viña, J. Role of nuclear glutathione as a key regulator of cell proliferation. *Mol. Aspects Med* **30:**77–85; 2009.

[66] Diaz Vivancos, P.; Dong, Y.; Ziegler, K.; Markovic, J.; Pallardó, F. V.; Pellny, T. K.; Verrier, P. J.; Foyer, C. H. Recruitment of glutathione into the nucleus during cell proliferation adjusts whole-cell redox homeostasis in Arabidopsis thaliana and lowers the oxidative defence shield. *Plant J* **64:**825–838; 2010.

[67] Markovic, J.; Mora, N. J.; Broseta, A. M.; Gimeno, A.; De-La-Concepción, N.; Viña, J.; Pallardó, F. V. The depletion of nuclear glutathione impairs cell proliferation in 3t3 fibroblasts. *PLoS One* **4:**e6413; 2009.

[68] Bourbouloux, A.; Shahi, P.; Chakladar, A.; Delrot, S.; Hgt1p, Bachhawat A. K. a high affinity glutathione transporter from the yeast Saccharomyces cerevisiae. *J. Biol. Chem.* **275:**13259–13265; 2000.

[69] Kaur, J.; Srikanth, C. V.; Bachhawat, A. K. Differential roles played by the native cysteine residues of the yeast glutathione transporter, Hgt1p. *FEMS Yeast Res* **9:**849–866; 2009.

[70] Rebbeor, J. F.; Connolly, G. C.; Dumont, M. E.; Ballatori, N. ATP-dependent transport of reduced glutathione on YCF1, the yeast orthologue of mammalian multidrug resistance associated proteins. *J. Biol. Chem* **273:**33449–33454; 1998.

[71] Jorgensen, P.; Edgington, N. P.; Schneider, B. L.; Rupes, I.; Tyers, M.; Futcher, B. The size of the nucleus increases as yeast cells grow. *Mol. Biol. Cell* **18:**3523–-3532; 2007.

[72] Durchschlag, E.; Reiter, W.; Ammerer, G.; Schüller, C. Nuclear localization destabilizes the stress-regulated transcription factor Msn2. *J. Biol. Chem.* **279:**55425–55432; 2004.

[73] Towpik, J.; Graczyk, D.; Gajda, A.; Lefebvre, O.; Boguta, M. Derepression of RNA polymerase III transcription by phosphorylation and nuclear export of its negative regulator, Maf1. *J. Biol. Chem* **283:**17168–17174; 2008.

[74] Pellicioli, A.; Foiani, M. Signal transduction: how rad53 kinase is activated. *Curr. Biol.* **15:**R769–R771; 2005.

[75] Lill, R.; Dutkiewicz, R.; Elsässer, H. -P.; Hausmann, A.; Netz, D. J. A.; Pierik, A. J.; Stehling, O.; Urzica, E.; Mühlenhoff, U. Mechanisms of iron–sulfur protein maturation in mitochondria, cytosol and nucleus of eukaryotes. *Biochim. Biophys. Acta* **1763:**652–667; 2006.